Transactions of Tianjin University (2021) 27:139–146
https://doi.org/10.1007/s12209-020-00279-z

RESEARCH ARTICLE

Single-Atom Pd–N_3 Sites on Carbon-Deficient g-C_3N_4 for Photocatalytic H_2 Evolution

Guimei Liu[1,2] · Haiqin Lv[1,3] · Yubin Zeng[2] · Mingzhe Yuan[1,3] · Qingguo Meng[1,3] · Yuanhao Wang[4] · Chuanyi Wang[1,2,3]

Received: 30 October 2020 / Revised: 20 November 2020 / Accepted: 3 December 2020 / Published online: 14 February 2021

Abstract

Photocatalytic hydrogen evolution is an attractive field for future environment-friendly energy. However, fast recombination of photogenerated charges severely inhibits hydrogen efficiency. Single-atom cocatalysts such as Pt have emerged as an effective method to enhance the photocatalytic activity by introduction of active sites and boosting charge separation with low-coordination environment. Herein, we demonstrated a new strategy to develop a highly active Pd single atom in carbon-deficient g-C_3N_4 with a unique coordination. The single-atom Pd–N_3 sites constructed by oil bath heating and photoreduction process were confirmed by HADDF-STEM and XPS measurements. Introduction of single-atom Pd greatly improved the separation and transportation of charge carriers, leading to a longer lifespan for consequent reactions. The obtained single-atom Pd loaded on the carbon-deficient g–C_3N_4 showed excellent photocatalytic activity in hydrogen production with about 24 and 4 times higher activity than that of g–C_3N_4 and nano-sized Pd on the same support, respectively. This work provides a new insight on the design of single-atom catalyst.

Keywords Single-atom · Pd · g-C_3N_4 · Active sites · Hydrogen · Photocatalytic

Introduction

Photocatalytic hydrogen evolution has been recognized as a promising approach to sustainable clean energy. Although much progress is made in improving photocatalysts' intrinsic activity, most photocatalysts still suffer from weak photo-absorption, limited active sites, and high charge-carrier recombination [1–5]. Among these adverse factors, the intrinsic nature of charge carriers' recombination is very critical, which makes limited photoelectrons access the reaction sites to reduce water for hydrogen production even with the presence of hole scavengers [6–9]. Therefore, modification with a cocatalyst turns out to be an effective alternative, aiming at significantly enhancing catalytic efficiency. Pt has proven to be one of the most promising cocatalysts, but its large-scale applications are limited by its scarcity and high price [1, 10]. Thus, it is necessary to develop alternatives or reduce Pt loading to improve hydrogen production.

Recently, single-atom sites on metal oxide [11, 12], N-doped carbon supports [13, 14], and graphite carbon nitride [15, 16] have been proposed as active sites for various reactions by downsizing metal particles [17]. The finely dispersed isolated metal atoms coordinated by metal or nonmetal atoms can be a promising ideal cocatalyst, which can not only minimize the use of noble metal, but also serve as active sites through exposure to low-coordination environment of metal centers [18, 19]. For example, Chen et al. [20] reported that Ag single atom supported on g-C_3N_4 in the coordination of Ag–N_2 exhibited an H_2 production of 1.87 mmol/(g·h). Such performance was as excellent as

✉ Yubin Zeng
zengyubin@whu.edu.c

✉ Mingzhe Yuan
mzyuan@sia.cn

✉ Chuanyi Wang
wangchuanyi@sust.edu.cn

1 Shenyang Institute of Automation, Guangzhou, Chinese Academy of Science, Guangzhou 511400, China

2 Hubei Key Laboratory of Accoutrement Technique in Fluid Machinery and Power Engineering, Hubei 430072, China

3 Guangdong Engineering Technology Research Center for Environmental Purification and Functional Materials, Guangzhou 511400, China

4 SUSTech Engineering Innovation Center, School of Environmental Science and Engineering, Southern University of Science and Technology, Shenzhen 518000, China

nano-Pt loaded on g-C_3N_4. Therefore, desirable hydrogen production performance could be achieved by reasonably regulating the coordination environment of metal cocatalyst.

The specific geometric and electronic structures of the single atom can regulate the catalytic activity of anchored single metal sites, especially for N, which acts as the coordination element. Indeed, the isolated metal–N_4 sites with porphyrin units were intensively studied, such as Fe–N_4 [21, 22], Ru–N_4 [23], Ni–N_4 [24], and Cu–N_4 [25] sites. Li et al. [26] reported that the isolated bond-shrinking low-valence Cu (+1)–N_4–C_8S_2 atomic interface moiety served as an active site for ORR process. Similarly, it has been found that Fe–N_4 center presented higher ORR efficiency after its surrounding charges were altered by S doping [27]. Other configurations including metal–N_2, metal–N_3, and metal–N_x sites are relatively less reported. Chen et al. [20] demonstrated that Ag–N_2 sites showed higher activity compared with Ag–N_4 sites for hydrogen production. In addition, Pt–N_3 single site was reported exhibited photocatalytic N_2 fixation ability [18]. Fu et al. [25] also observed that the complex of Cu–N_3 and Cu–N_4 could boost the hydrogen yield. It is worth mentioning that the construction of Pd–N_3 coordination structure in g-C_3N_4 acting as photocatalytic sites has not yet been reported, which could provide ideal unoccupied N atoms once the carbon in the s-triazine rings was removed.

In this work, we successfully anchored single-atom Pd–N_3 sites on carbon-deficient g–C_3N_4, which showed intriguing photocatalytic H_2 evolution activity compared to its counterparts. The isolated sites were confirmed by XPS and HAADF-STEM measurements, and the mechanism was discussed in detail.

Experimental Section

Preparation of Carbon-Deficient g–C_3N_4

Put 10 g of urea into a 50-mL crucible with a cover. It was then transferred to the muffle furnace and kept at 600 °C for 2 h. The final product was ground into powder and denoted as CN.

Synthesis of Single-Atom Pd Loaded on Carbon-Deficient g-C_3N_4

0.3 g CN was added into 100 mL of deionized water. Then, 0.5 mL solution of $PdCl_2$ (1 mg/ mL) and NaCl (5 mg/mL) was dissolved into the above suspension after being thoroughly mixed by an ultrasonic cell disruptor for 30 min. The obtained mixture was then constantly stirred at 80 °C for 8 h in an oil bath. After cooling to ambient temperature, the mixture was washed with deionized water several times. The remaining mixture was dispersed with 100 mL deionized water and radiated under 300 W Xe lamp for 1 h. The final product was washed with deionized water and dried in the freezer drier overnight. The final sample was denoted as Pd–CN.

Preparation of Nano-Sized Pd Loaded on Carbon-Deficient g-C_3N_4

The nano-sized Pd loaded on CN was prepared by a similar route: 4 mL solution of $PdCl_2$ (1 mg/mL) and NaCl (5 mg/mL) was dissolved into suspension of 100 mL deionized water and 0.3 g CN. Then, the mixture was stirred under illumination by the 300 W Xe lamp for 3 h. The final product was washed with deionized water and dried in the freezer drier overnight. The final sample was denoted as Pd_{nano}-CN.

Characterization

Transmission electron microscopy (TEM) observations and energy-dispersive X-ray spectroscopy mapping images were obtained using a Titan G2 60–300 microscope. Aberration-corrected HAADF-STEM characterization was performed on a Cs-corrected Titan G2 60–300 electron microscope (FEI, USA). X-ray diffractions were conducted to identify crystal phases by a D8 Rigaku9000 using a Cu Kα radiation in the 2θ range of 5°–80°. Fourier transform infrared spectra (FTIR) were recorded on a NICOLET iS10 FTIR spectrometer. X-ray photoelectron spectroscopy (XPS) was performed on a Thermo Scientific K-Alpha + spectrometer. UV–Vis diffuse reflectance spectra (UV–Vis DRS) were achieved on a UV-8000A system. Photoluminescence (PL) and time-resolved transient PL decay spectroscopic analyses were conducted by an Edinburgh FLS1000 spectrophotometer with an excitation wavelength of 360 nm.

Photocatalytic Hydrogen Evolution

Photocatalytic hydrogen evolution was tested in a typical route: 15 mg of the sample was dispersed in a 100 mL aqueous solution with 5 vol% triethanolamine (TEOA) as the hole scavenger. After bubbled with N_2 to remove the oxygen for 30 min, the test was carried out using 300 W Xe light under 5 °C and atmospheric pressure. The amount of H_2 was determined by gas chromatography (SHIMADZU GC-2014C). The apparent quantum yield (AQY) for hydrogen evolution was estimated as follows: $AQY = 2n_{H2}N_A/N_{photon} \times 100\%$, where the n_{H2} refers to the mole amount of produced H_2 molecules, N_A refers Avogadro constant, and the N_{photon} corresponds to the amount of photons. The cycling test was similarly conducted in a typical route: after the first experiment, the light source was turned off and N_2 was bubbled into the reactor to remove the hydrogen for 30 min. The

experiment was restarted by turning on the light, and the next cycling was conducted similarly.

Results and Discussion

Synthesis and Characterizations of Pd–CN

Among different coordination elements, N is the most accessible for N-based materials providing strong anchoring sites for single-atom loading. g-C_3N_4 is an ideal support since its s-triazine rings are rich in N despite being bonded to carbon atoms. The carbon-deficient g-C_3N_4 was prepared following a protocol developed by our group previously [28]. Its C/N molar ratio fell from 0.75 (the ideal ratio) to 0.66 according to the XPS spectral analysis, while the ratio for bulk g-C_3N_4 was 0.72 as confirmed by elemental analysis (Table 1), signifying successful introduction of carbon defects. The carbon-deficient g-C_3N_4 served as a perfect carrier, owning to its three unoccupied N atoms. After pre-absorption and photoreduction of Pd^{2+}, the Pd supported on CN can be obtained as illustrated in Fig. 1a. HADDF-TEM images in Fig. 1b reveal uniform dispersion of the Pd element on the surface of CN. Figure 1c confirms the atomically dispersed Pd, which suggests that the single-atom Pd was successfully obtained.

Table 1 Elemental analysis

Photocatalyst	N atom (%)	C atom (%)	C/N molar ratio
Bulk g-C_3N_4	59.70	36.79	0.72
CN	58.55	32.95	0.66

XRD spectra of Pd–CN in Fig. 2a reveal two characteristic peaks at 27.8° and 13.0°, corresponding to the (002) and (100) crystal plane of graphite phase carbon nitride, respectively. No changes in the position and shape of these two peaks were observed with the addition of single-atom Pd compared to its counterparts, CN and Pd_{nano}–CN, indicating that the triazine ring structure remained the same with CN after introduction of Pd. This is also confirmed by FTIR spectral measurement.

XPS was conducted to explore more information about surface composition of CN, Pd–CN, and Pd_{nano}–CN. Four elements including C, N, O, and Pd were found in the Pd-loaded samples (Fig. 3), which are in accordance with the results of HADDF-STEM. The binding energy peaks at 285 eV and 288 eV obtained from Pd–CN can be assigned to the adventitious carbon and C-N_3 in typical aromatic C_3N_4 heterocycles, respectively. The N 1s peaks in Fig. 3b can be resolved into three peaks centered at 398, 400, and 401 eV, which are related to C=N–C, N–C_3, and $-NH_x$ ($x = 1, 2$), respectively. O originated from the N–C–O corresponding to lattice oxygen in the bulk located at 532 eV [29]. Noticeably, two different forms of Pd can be seen in the Pd–CN, namely Pd^+ and Pd^{2+} located between 336.8 and 342.0 eV and between 338.0 and 343.2 eV, respectively [30, 31]. However, metallic Pd^0 can only be observed for Pd_{nano}–CN, which is located at 335.2 eV and 340.5 eV (Fig. 3d). This

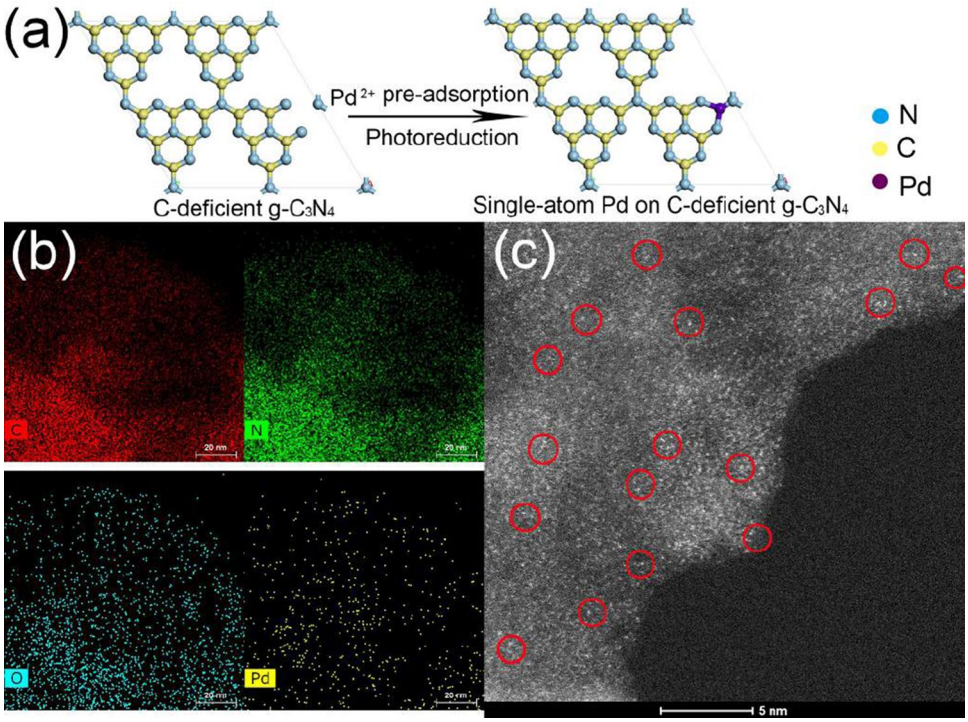

Fig. 1 **a** Illustration of single atom loaded on carbon-deficient g–C_3N_4, **b** HADDF-TEM images of Pd–CN, and **c** representative aberration-corrected HAADF-STEM of Pd–CN. The red circles were drawn around the single-atom Pd

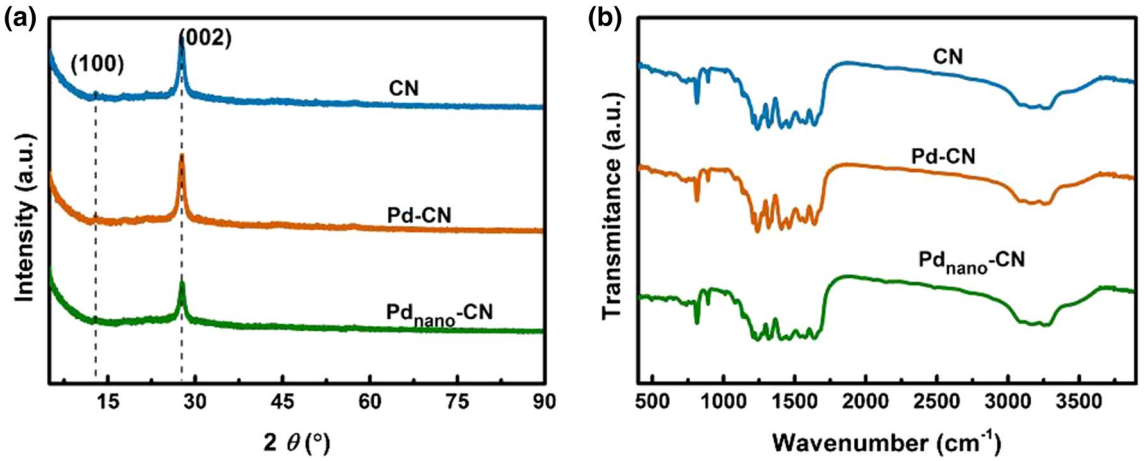

Fig. 2 **a** XRD patterns and **b** FTIR spectra of CN, Pd–CN, and Pd_{nano}–CN

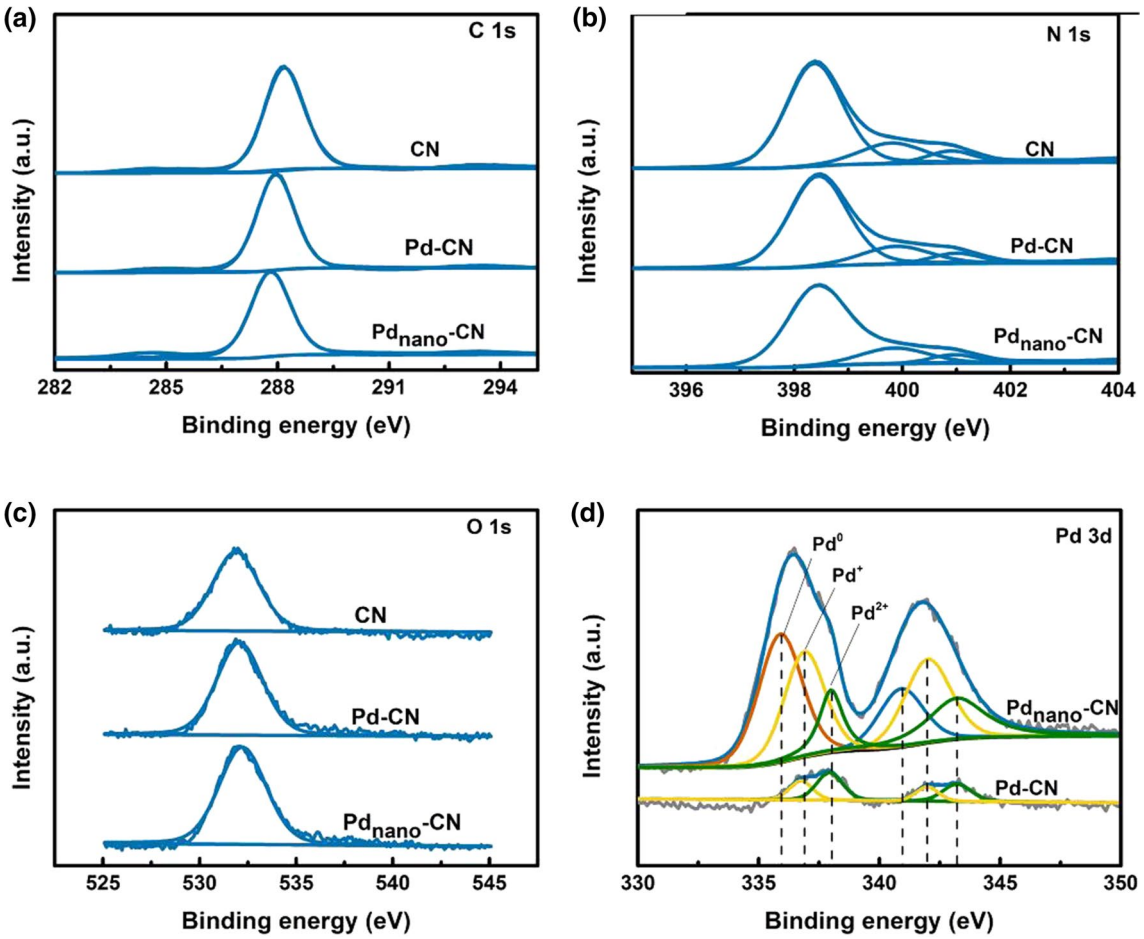

Fig. 3 **a** C 1 s, **b** N 1 s, **c** O 1 s, and **d** Pd 3d XPS spectra of CN, Pd–CN, and Pd_{nano}–CN

also proves that Pd was introduced in the form of single atom instead of nanoparticle. Furthermore, the peaks of Pd^{2+} significantly shifted to lower binding energy, compared with the Pd precursor (338.4 eV and 343.7 eV) [15]. In addition, Pd^{2+} peaks approximated to the shapes and positions of Pd–N coordination (337.2 eV and 342.5 eV) as reported

previously [32], suggesting bonding of the single-atom Pd with nearby N atoms. HADDF-STEM and XPS results demonstrated that the atomically dispersed Pd was coordinated with carbon vacancy-resulted N (Pd–N_3) in CN. Loading of the single atom on the carbon defects instead on the pore is attributed to ligand–metal charge transfer (LMCT) coordination effect. Wang et al. [28] reported similar observation, suggesting that the Pd–N_3 sites on C-deficient g-C_3N_4 were energetically more favorable.

Photocatalytic Activity and Mechanism Analysis

Samples were tested for hydrogen evolution activity in an aqueous sacrificial solution containing triethanolamine (TEOA). The fully optimized results are shown in Fig. 4a. Pd–CN exhibited superior hydrogen evolution in comparison with CN and Pd_{nano}–CN under full arc irradiation. The Pd–CN evolved hydrogen at approximately 2788 μmol/(g·h), which is 4 times faster than Pd_{nano}–CN, indicating that the single-atom Pd has higher activity toward H_2 production. Photocatalytic activities of the samples under two different specific wavelengths of light ($\lambda = 420$ nm, 380 nm) were also investigated. As seen in Fig. 4b, Pd–CN showed higher apparent quantum efficiency of H_2 evolution under ultraviolet irradiation compared to CN and Pd_{nano}–CN. These results proved the excellent activity of Pd–CN for photocatalytic H_2 evolution. The long-term photocatalytic stability was tested in three cycles. As seen in Fig. 4c, Pd–CN remained stable under continuous irradiation and its performance did not decrease significantly.

Light absorption in Fig. 5a increased in the range of 500–800 nm as Pd particle grew. As illustrated in Fig. 5b, the band gap remained the same with CN, but the valence band (VB) position decreased significantly with the introduction of Pd atom (Fig. 5c). As a result, conduction band (CB) shifted to a more negative position, which suggests enhanced reduction capability. By contrast, Pd_{nano}–CN showed enhanced visible light absorption and a narrowed band gap. It is worth mentioning that these advantages for Pd_{nano}–CN did not make much contribution to the H_2 production. Otherwise, it should have performed better than Pd–CN, which also suggests that the single atom is more advantageous.

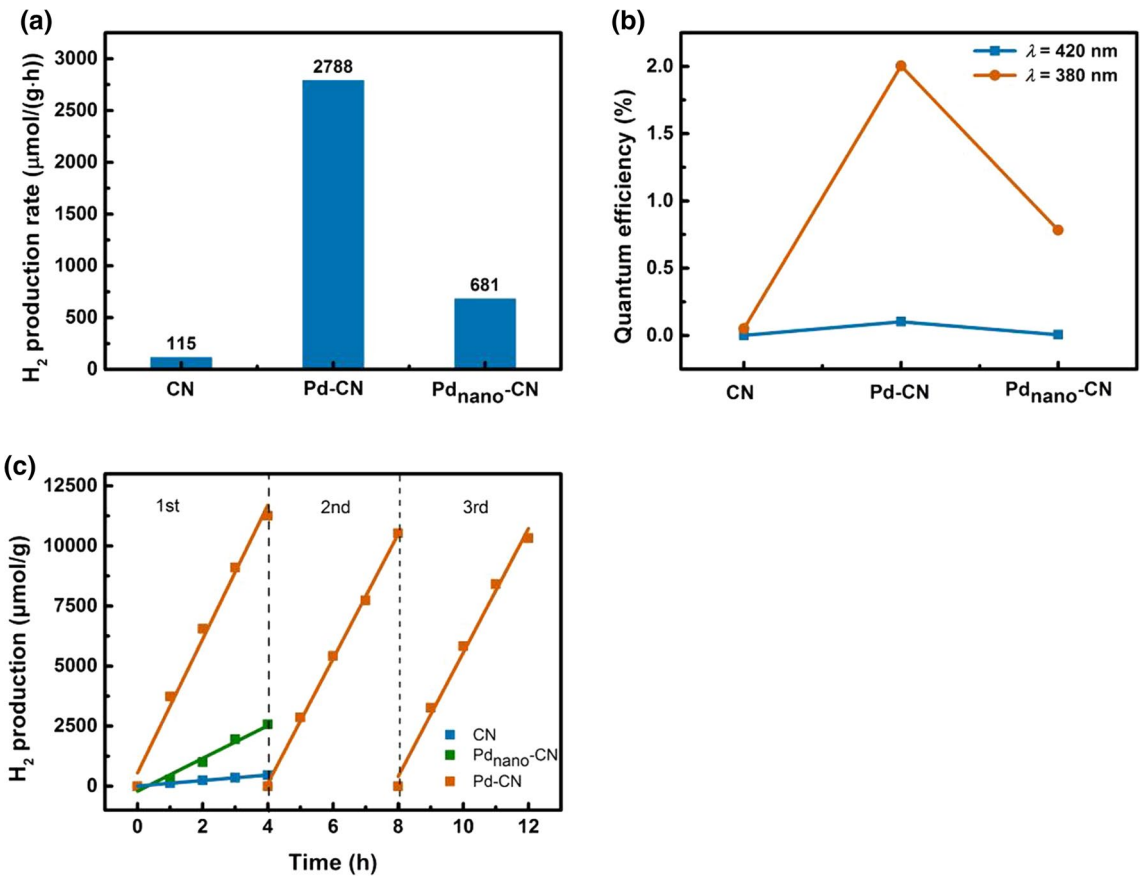

Fig.4 **a** Photocatalytic H_2 production activity; **b** quantum efficiency of CN, Pd–CN and Pd_{nano}–CN; **c** cycling runs of photocatalytic H_2 production for Pd–CN

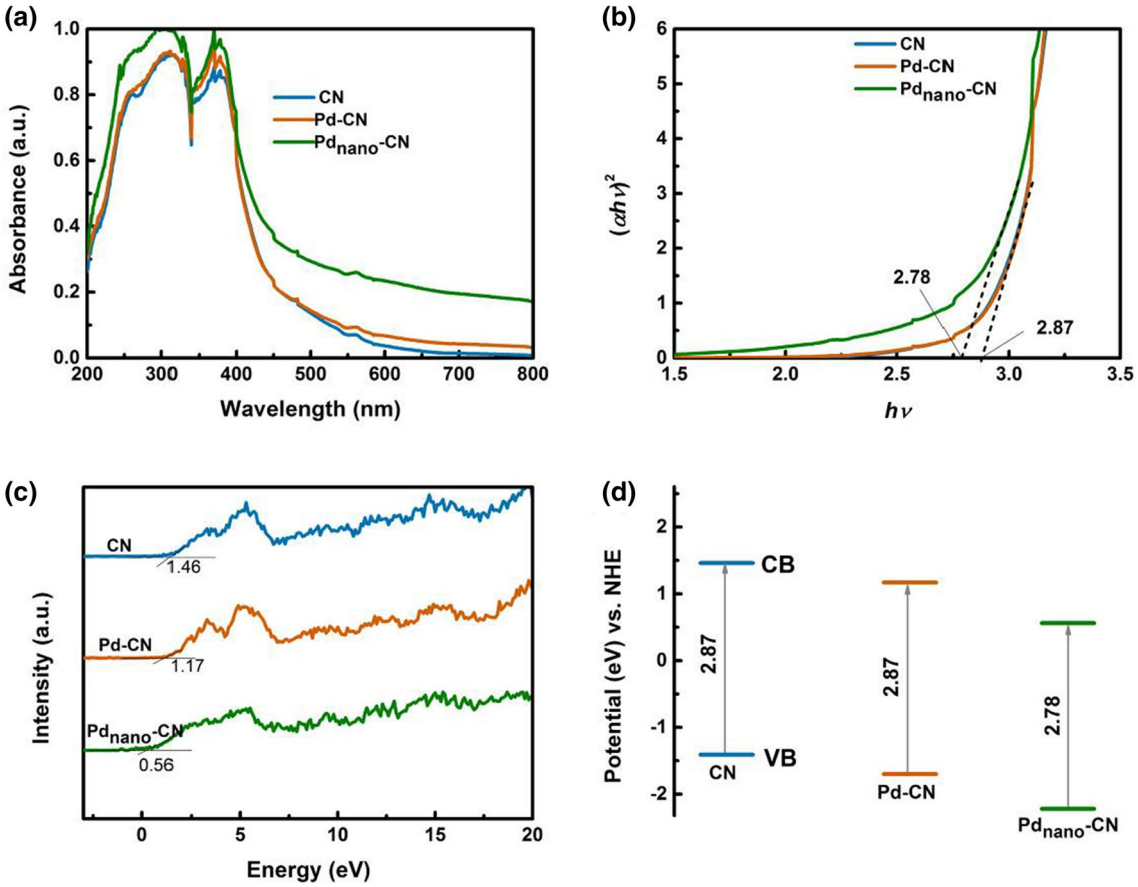

Fig.5 **a** UV–Vis diffuse reflectance spectra, **b** estimated band gaps, **c** VB XPS, **d** schematic illustration of the band gap structure of CN, Pd–CN, and Pd_{nano}–CN

The charge transfer ability of Pd–CN was demonstrated by combining the analysis of steady-state and time-resolved photoluminescence (TRPL) spectroscopy with the CN benchmark as a reference. The steady-state PL spectra showed that the intrinsic emission peak of CN was greatly weakened by introduction of Pd, implying a lower charge recombination rate in Pd–CN and Pd_{nano}–CN (Fig. 6a). A customized time-correlated single-photon counting apparatus was employed in the collection of the TRPL spectra (Fig. 6b) to gain a deep insight into the charge-transfer

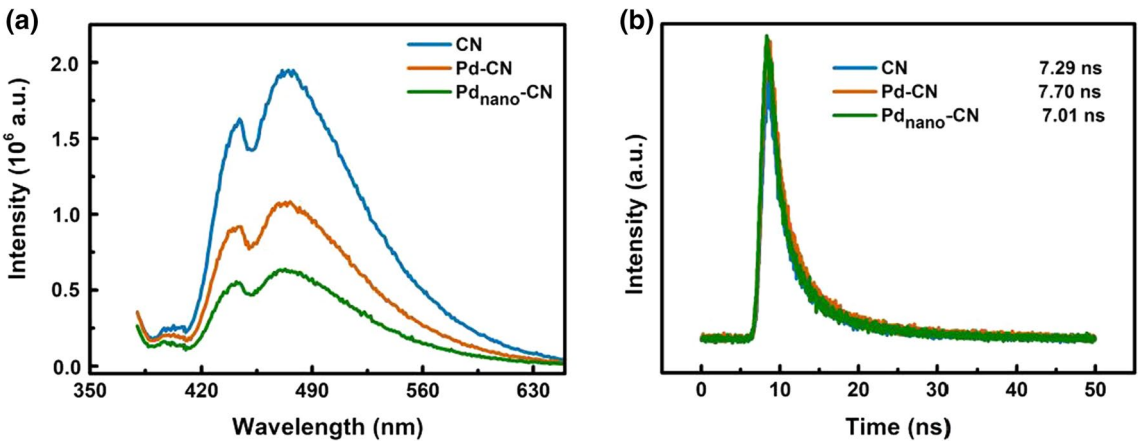

Fig. 6 **a** Steady-state PL spectra, **b** time-resolved PL spectra of CN, Pd–CN, and Pd_{nano}–CN

dynamics, where a biexponential fitting is applied to analyze the luminescence decay curves due to their complexity. Obviously, in contrast to CN, the lifetime of charge carriers was prolonged for Pd–CN (7.70 ns), whereas that for Pd_{nano}–CN (7.01 ns) was shortened, elucidating that single-atom Pd loaded on CN can enhance the charge transfer and separation. However, shorter lifetime was observed in Pd_{nano}–CN, which means that nano-Pd can transfer to be combination centers rather than active sites. As a result, the photocatalytic activity is dropped with the nano-sized Pd loading compared to single-atom Pd loading.

Conclusion

In summary, a strategy based on deficient carbon structure was applied to develop single-atom Pd–N_3 sites. The HADDF-STEM and XPS measurements supported that the single-atom Pd was successfully loaded on the carbon-deficient g–C_3N_4 in the form of isolated Pd–N_3 sites. The addition of single-atom Pd improved the photogenerated charge carriers' separation and transfer, leading to remarkably improved performance of photocatalytic H_2 evolution compared to its counterparts, the addition of loading nano-sized Pd and pristine g–C_3N_4.

Acknowledgements This work was supported by the National Natural Science Foundation of China (Nos. 21976116, 21473248); Guangdong Science and Technology Program (No. 2018A050506025); Guangzhou Science and Technology Program (Nos. 202002030406, 201804010181); High Level Talents Introduction Project of "Pearl River Talent Plan" in Guangdong Province (No. 2019CX01L308); the Support Scheme of Guangzhou for Leading Talents in Innovation and Entrepreneurship Funding (No. 2016015); and the Key Deployment Projects of Chinese Academy of Sciences (No. ZDRW_CN_2020_1).

References

1. Cao YJ, Wang DH, Lin Y et al (2018) Single Pt atom with highly vacant d-orbital for accelerating photocatalytic H_2 evolution. ACS Appl Energy Mater 1(11):6082–6088
2. Ran JR, Ma TY, Gao GP et al (2015) Porous P-doped graphitic carbon nitride nanosheets for synergistically enhanced visible-light photocatalytic H_2 production. Energy Environ Sci 8(12):3708–3717
3. Zhang JH, Wei MJ, Wei ZW et al (2020) Ultrathin graphitic carbon nitride nanosheets for photocatalytic hydrogen evolution. ACS Appl Nano Mater 3(2):1010–1018
4. Gao JF, Zhang FD, Xue HQ et al (2021) In-situ synthesis of novel ternary CdS/PdAg/g-C_3N_4 hybrid photocatalyst with significantly enhanced hydrogen production activity and catalytic mechanism exploration. Appl Catal B: Environ 281:119509
5. Kim D, Yong K (2021) Boron doping induced charge transfer switching of a C_3N_4/ZnO photocatalyst from Z-scheme to type II to enhance photocatalytic hydrogen production. Appl Catal B: Environ 282:119538
6. Chen ZW, Bu YY, Wang L et al (2020) Single-sites Rh-phosphide modified carbon nitride photocatalyst for boosting hydrogen evolution under visible light. Appl Catal B: Environ 274:119117
7. Wang X, Zhang YW, Si HN et al (2020) Single-atom vacancy defect to trigger high-efficiency hydrogen evolution of MoS_2. J Am Chem Soc 142(9):4298–4308
8. Wang YY, Zhao S, Zhang YW et al (2018) Facile synthesis of self-assembled g-C_3N_4 with abundant nitrogen defects for photocatalytic hydrogen evolution. ACS Sustain Chem Eng 6(8):10200–10210
9. Qiu CH, Bai S, Cao WJ et al (2020) Tunable syngas synthesis from photocatalytic CO_2 reduction under visible-light irradiation by interfacial engineering. Trans Tianjin Univ 26(5):352–361
10. Li XG, Bi WT, Zhang L et al (2016) Single-atom Pt as Co-catalyst for enhanced photocatalytic H_2 evolution. Adv Mater 28(12):2427–2431
11. Xin P, Zhao Y, Qin RX et al (2016) Photochemical route for synthesizing atomically dispersed palladium catalysts. Science 352(6287):797–801
12. Lee BH, Park S, Kim M et al (2019) Reversible and cooperative photoactivation of single-atom Cu/TiO_2 photocatalysts. Nat Mater 18(6):620–626
13. Lu PL, Yang Y, Yao JN et al (2019) Facile synthesis of single-nickel-atomic dispersed N-doped carbon framework for efficient electrochemical CO_2 reduction. Appl Catal B 241:113–119
14. Geng ZG, Liu Y, Kong XD et al (2018) Achieving a record-high yield rate of 120.9 μgNH3 mgcat.-1 h-1 for N2 electrochemical reduction over Ru single-atom catalysts. Adv Mater. 30(40):1803498
15. Cao SW, Li H, Tong et al (2018) Photocatalysis: single-atom engineering of directional charge transfer channels and active sites for photocatalytic hydrogen evolution. Adv Funct Mater 28(32):1870224
16. Chen ZP, Vorobyeva E, Mitchell S et al (2018) Single-atom heterogeneous catalysts based on distinct carbon nitride scaffolds. National Science Review 5:642–652
17. Yang XF, Wang AQ, Qiao BT et al (2013) Single-atom catalysts: a new frontier in heterogeneous catalysis. Acc Chem Res 46(8):1740–1748
18. Liu KP, Zhao XT, Ren GQ et al (2020) Strong metal-support interaction promoted scalable production of thermally stable single-atom catalysts. Nat Commun 11:1263
19. Dong CY, Lian C, Hu SC et al (2018) Size-dependent activity and selectivity of carbon dioxide photocatalytic reduction over platinum nanoparticles. Nat Commun 9:1252
20. Jiang XH, Zhang LS, Liu HY et al (2020) Silver single atom in carbon nitride catalyst for highly efficient photocatalytic hydrogen evolution. Angew Chem Int Ed Engl 59:1–6

21. Zhang CH, Yang SZ, Wu JJ et al (2018) Electrochemical CO_2 reduction with atomic iron-dispersed on nitrogen-doped graphene. Adv Energy Mater 8(19):1703487
22. Wan X, Liu XF, Li YC et al (2019) Fe–N–C electrocatalyst with dense active sites and efficient mass transport for high-performance proton exchange membrane fuel cells. Nat Catal 2(3):259–268
23. Hu XL, Luo G, Zhao QN et al (2020) Ru single atoms on N-doped carbon by spatial confinement and ionic substitution strategies for high-performance Li–O_2 batteries. J Am Chem Soc 142(39):16776–16786
24. Zhao SY, Chen GX, Zhou GM et al (2020) A universal seeding strategy to synthesize single atom catalysts on 2D materials for electrocatalytic applications. Adv Funct Mater 30(6):1906157
25. Xiao XD, Gao YT, Zhang LP et al (2020) A promoted charge separation/transfer system from Cu single atoms and C_3N_4 layers for efficient photocatalysis. Adv Mater 32(33):2003082
26. Jiang ZL, Sun WM, Shang HS et al (2019) Atomic interface effect of a single atom copper catalyst for enhanced oxygen reduction reactions. Energy Environ Sci 12(12):3508–3514
27. Li QH, Chen WX, Xiao H et al (2018) Fe isolated single atoms on S, N codoped carbon by copolymer pyrolysis strategy for highly efficient oxygen reduction reaction. Adv Mater 30(25):1800588
28. Liu GM, Huang Y, Lv H et al (2021) Confining single-atom Pd on g-C_3N_4 with carbon vacancies towards enhanced photocatalytic NO conversion. Appl Catal B Environ 84:119683
29. Martin DJ, Qiu KP, Andrew S et al (2014) Highly efficient photocatalytic H_2 evolution from water using visible light and structure-controlled graphitic carbon nitride. Angew Chem Int Ed 53(35):9240–9245
30. Sharma P, Sasson Y (2019) Sustainable visible light assisted in situ hydrogenation via a magnesium–water system catalyzed by a Pd-g-C_3N_4 photocatalyst. Green Chem 21(2):261–268
31. Xu XL, Luo JJ, Li LP et al (2018) Unprecedented catalytic performance in amine syntheses via Pd/g-C_3N_4 catalyst-assisted transfer hydrogenation. Green Chem 20(9):2038–2046
32. Arrigo R, Schuster ME, Xie ZL et al (2015) Nature of the N-Pd interaction in nitrogen-doped carbon nanotube catalysts. ACS Catal 5(5):2740–2753

Yubin Zeng obtained her PhD degree from Department of Environmental Science and Engineering, Huazhong University of Science and Technology, China, in 2007. She worked in Korea (Department of Civil and Environmental Engineering, Seoul National University) as a postdoctor fellowship with Prof. Junboum Park from 2008 to 2009. Currently, she is an associate professor at Wuhan University, China. Her research interest mainly focuses on environmental photocatalysis.

Mingzhe Yuan is a researcher of Shenyang Institute of Automation, Guangzhou, Chinese Academy of Science (CAS). He obtained his PhD degree from Shenyang Institute of Automation of CAS in 2006. Currently, his research interest covers functional materials and environmental photocatalysis. By far, he has published over 100 papers in peer-reviewed journals.

Chuanyi Wang Fellow of Royal Society of Chemistry, is a distinguished professor of Chinese Academy of Sciences (CAS) and an adjunct professor at Wuhan University. He obtained his PhD degree from Institute of Photographic Chemistry of CAS in 1998, worked in Germany (Institute for Solar Energy Research in Hannover and Free University Berlin) as an Alexander von Humboldt research fellow with Prof. Detlef Bahnemann from 1999 to 2000, and then worked in USA (Tufts University and Missouri University-Kansas City) as a research faculty from 2000 to 2010. Currently, Dr. Wang also serves as an associate editor of Environmental Chemistry Letters and an editorial board member for number of international journals. His research interest covers eco-materials and environmental photocatalysis. By far, he has published over 200 papers in peer-reviewed journals.